# Catalysis Science & Technology

Accepted Manuscript






ROYAL SOCIETY OF CHEMISTRY

www.rsc.org/catalysis

# Nickel and Cobalt phosphide as effective catalysts for oxygen-removal of dibenzofuran: Role of contact time, hydrogen pressure and hydrogen/feed molar ratio

A. Infantes Molina[a*], E. Gralberg[a], J.A. Cecilia[a], Elisabetta Finocchio[b], E. Rodríguez-Castellón[a]

[a]*Departamento de Química Inorgánica, Cristalografía y Mineralogía (Unidad Asociada al ICP-CSIC), Facultad de Ciencias, Universidad de Málaga, Campus de Teatinos, 29071 Málaga (Spain)*

[b]*Dipartimento di Ingegneria Civile, Chimica ed Ambientale, Università di Genova, P.le J.F.Kennedy 1, 16129 Genova (Italy)*

*Corresponding Author: ainfantes@uma.es*

## Abstract

The catalytic activity of nickel- and cobalt phosphides, with a metallic loading of 5 wt.%, supported on silica was investigated in the hydrodeoxygenation reaction (HDO) of dibenzofuran (DBF) as model oxygenated compound at different contact times, $H_2$ pressures and $H_2$/DBF molar ratios. The aim of the study was to understand the mechanism of the reaction and to study the impact of $H_2$ pressure and $H_2$/DBF molar ratio on the reaction. The catalysts were characterized by $N_2$ adsorption–desorption isotherms at −196 °C, X-ray diffraction (XRD), X-ray photoelectron spectroscopy(XPS), CO-chemisorption, $NH_3$ Temperature-Programmed Desorption ($NH_3$-TPD), IR- Spectroscopy and $H_2$ Temperature-Programmed Desorption ($H_2$-TPD). The prepared catalysts were tested in the HDO reaction of DBF in a continuous-flow fixed-bed stainless steel catalytic reactor at pressures ranging from 1-30 bars at 275 °C. The results obtained indicate that the $Ni_2P$ catalyst is more active than the CoP catalyst, converting more than 90% of the DBF at the highest contact time into oxygen-free products. The activity of both catalysts increases with increased contact time. At low contact times the intermediates tetrahydrodibenzofuran (THDBF) and hexahydrodibenzofuran (HHDBF) are observed as products, while an increment in the contact time led to the transformation of THDBF and HHDBF into O-free compounds, mainly bicyclohexane (BCH), indicating that the HDO of DBF follows the path: DBF → HHDBF → THDBF → 2-CHP → BCH. Further both $Ni_2P$ and CoP catalysts are active at medium pressures with HDO degrees similar to those obtained at 30 bar. $Ni_2P$ is less affected by changes in $H_2$/DBF ratio than CoP and the catalysts are more active at high $H_2$/DBF molar ratios.

***Keywords:*** HDO; $Ni_2P$; CoP; Dibenzofuran; Silica; transition metal phosphides

## 1. Introduction

The use of bioenergy as a renewable alternative to fossil fuels is nowadays attracting more and more attention. The reasons are quite obvious: our world is running out of oil reserves; the raw oil quality is decreasing;[1] and the world petroleum consumption continues to rise as a consequence of the world's high population growth, the industrialization and a big change in consumption pattern. Within this scenario, biofuels seem to be a potential energy substitute for fossil fuels since it is a renewable resource that could contribute to sustainable development and global environmental preservation[2].

Bio-oil is formed from fast pyrolysis of biomass. It retains most of the original oxygen in the feedstocks and the oxygen content varies in the range of 35-60 wt.% on a wet basis. First of all, the oxygenated compounds make the bio-oil polar and for this reason it will be non-miscible with non-polar petroleum fuels. The high oxygen content also gives the bio-oil other important undesirable properties. Hence, upgrading is necessary to use the pyrolysis-oil as a competitive substitute of petroleum fuels. Most important is a de-oxygenation step prior to co-processing[3, 4].

HDO is a promising future process for the up-grading of bio-oil. The HDO process requires the presence of hydrogen and a catalyst, and it normally operates at moderate temperatures, up to 450 °C and at a high pressure, 10-300 bar. The high pressure increases the reaction rate and decreases the formation of coke in the reactor. A good HDO catalyst should be highly active to remove oxygen in the bio-oil with a high yield and it should not produce coke[5].

HDO is a process very similar to HDS and commercial catalysts, often used for traditional hydrotreating processes such as Co-$MoS_2$ and Ni-$MoS_2$ supported on ©-$Al_2O_3$, have been the most frequently tested catalysts also for HDO reactions.[6] However a problem with the above named catalysts is that co-feeding of $H_2S$ is needed in order to regenerate the sulphide sites. Further the sulphidation agent must be separated from the products and the sulphur must be recovered from the $H_2S$. Another disadvantage is the corrosiveness of $H_2S$[7].

Noble metal supported catalysts as for example Ru/C and Pt/C have also shown good results in HDO reactions. Noble metal catalysts in HDO are also active at low temperatures. However, the main disadvantages with noble metal based catalysts are their high cost and additionally they show a low resistance towards poisoning by the presence of sulphur[8].

Alternative compositions that show good hydrogen transferring properties are metal carbides, metal nitrides, metal borides and transition metal phosphides[9]. Transition metal phosphides have

presented very interesting properties in hydrotreating reactions as they are bifunctional with acid and metallic catalytic functions. The metallic function is responsible for hydrogenation, while on the acidic sites, hydrogenolysis, dehydration, and isomerization reactions take place. The balance among these functions determines the observed catalytic activity. From FTIR studies of CO adsorption of the transition metal phosphide $Ni_2P/SiO_2$, it has been shown that there are enough electrons on the metal site to allow π-back bonding. This π-back bonding enables molecular activation as electrons fill antibonding orbitals and the hydrogenation activity is thereby enhanced. The acidity arises from acidic PO-H sites[10].

In the last decade a series of studies have shown that MoP, WP, $Fe_2P$, CoP and $Ni_2P$ are suitable for hydrodesulfurization and hydrodenitrogenation of fossil crude oils[11-15] . More recently, these transition metal phosphides have also been applied as catalysts in HDO reactions of bio-oil [16, 17] as they show good hydrogen transfer properties. These kinds of catalysts are favored when supported on a less acidic support as silica, SBA-15 or MCM-41. Zhao et al.[18] measured the activity for the HDO reaction of guaiacol over $Ni_2P$, $Co_2P$, $Fe_2P$, WP and MoP catalysts supported on $SiO_2$ in a fixed bed reactor with a molar ratio $H_2$/guaiacol of 33. The results indicated that the type of metal has a significant effect on product distribution and a different involvement of metals during the hydrogen activation or the interaction of reactants with the catalyst surface were suggested. The activity of the different catalyst followed the order: $Ni_2P$ >$Co_2P$ >$Fe_2P$≈WP≈MoP. The activities of the transition metal catalysts were compared to the catalytic activity of the commercial catalyst $CoMoS/Al_2O_3$ and $5\%Pd/Al_2O_3$. The commercial 5% $Pd/Al_2O_3$ catalyst turned out to be more active than the metal phosphides at lower contact time, but the major product was catechol which is undesired. A. Iino et al.[19] studied the HDO reaction of 2-metyltetrahydrofuran (2-MTHF) on a $Ni_2P/SiO_2$ catalyst with a continuous-flow quartz reactor. The activity and selectivity of this transition metal phosphide catalyst were compared to $Pd/Al_2O_3$ and Ru/C catalysts. The results showed that $Ni_2P/SiO_2$ had higher selectivity to *n*-pentane and lower selectivity to lower hydrocarbons with carbon numbers less than 5 compared to $Pd/Al_2O_3$ and Ru/C. It was concluded that $Ni_2P/SiO_2$ catalyst has high HDO activity and low carbon bond cracking propensity.

When it comes to the reaction parameters, Mortensen et al.[20] describe in their review of catalytic upgrading of bio-oil that a high pressure is beneficial in the HDO process. A high pressure increases the solubility of hydrogen in the oil and consequently there will be higher availability of hydrogen in the proximity to the catalyst. This increases the reaction rate and counteracts carbon deposition on the surface of the catalyst. However, a great amount of hydrogen interferes with

the adsorption of reactant on the surface[19]. In the work of A. Iino et al.[19] the results showed that the conversion decreases as $H_2$ partial pressure increases. These experiments were run under $H_2$ partial pressures in the range 75-418 kPa. In a recent study of T.A. Le et al.[21] the HDO process of 2-furyl methyl ketone (FMK) catalyzed by CoP/γ-$Al_2O_3$, the complete HDO of FMK into methyl cyclopentane and methane was achieved at 400 °C and at atmospheric pressure. The authors urge that positive catalytic results can be achieved even at atmospheric pressure (low pressure).

In this work, the focus is on the activity of nickel phosphide catalyst ($Ni_2P$) and cobalt phosphide catalyst (CoP), both supported on silica and tested in the HDO of dibenzofuran (DBF). In a previous work the HDO of DBF on $Ni_2P$ with different metallic loadings and P/Ni molar ratios was studied. In the present paper an evaluation of the impact of the experimental parameters on the catalytic response of these catalysts is carried out (contact time, $H_2$ pressure and $H_2$/DBF molar ratio) to better understand the reaction mechanism of the two phosphide-type catalysts.

## 2. Experimental

### *2.1. Materials*

The catalytic support used in this study was commercial fumed silica from Sigma-Aldrich. The reagents used for the preparation of the precursor solution were nickel(II) hydroxide ($Ni(OH)_2$), cobalt(II) hydroxide ($Co(OH)_2$, 95%) and phosphorous acid ($H_2PO_3H$, 99%), all supplied by Sigma Aldrich. In the catalytic reactivity study the chemicals used were dibenzofuran($C_{12}H_8O$, 98%) and decahydronaphtalene, cis+trans ($C_{10}H_{18}$, 98%), both from Alfa Aesar. The gases used in the experimentation, $H_2$, $N_2$, CO, $NH_3$ had a purity of 99.9999% and were supplied by Air Liquide.

### *2.2. Preparation of catalysts*

Nickel phosphide and cobalt phosphide catalysts containing 5 wt.% of nickel and cobalt, respectively, supported on fumed commercial silica ($S_{BET}$ = 218 $m^2$ $g^{-1}$ and Vp = 0.52 $cm^3$ $g^{-1}$) were prepared. Precursor solutions of nickel(II) dihydrogenphosphite ($Ni(HPO_3H)_2$) and cobalt(II) dihydrogenphosphite ($Co(HPO_3H)_2$) were prepared as described elsewhere[14, 15]. The precursor solutions were incorporated into the silica support by the incipient wetness impregnation method to prepare catalysts containing 5 wt.% of metal. To convert the precursor phosphite into phosphide the impregnated solids were dried at 60°C for 24 hours and treated in hydrogen by heating at a linear temperature ramp (3 ºC $min^{-1}$) in flowing $H_2$ (100 ml $min^{-1}$), from rt. to 620 ºC for nickel phosphide catalysts and from rt. to 700 ºC for cobalt phosphide catalysts. The obtained catalysts will hereafter be named as $Ni_2P$ and CoP.

### *2.3. Characterization of catalysts*

The textural properties ($S_{BET}$, $V_p$, $d_p$) of the fresh catalysts were obtained from the $N_2$ adsorption-desorption isotherms at -196 ºC measured with a Micromeritics ASAP 2020 apparatus. Prior to the measurements the samples were outgassed at 200 ºC and 0.01 kPa overnight. Surface areas were determined by using the Brunauer-Emmet-Teller equation and a nitrogen molecule cross section of 16.2 $Å^2$ (3). The pore size distribution was calculated by applying the Barrer-Joyner-Halenda method (BJH) to the desorption branch. The total pore volume was calculated from the adsorption isotherm at $P/P_0 = 0.95$.

X-ray diffraction patterns (XRD) of the samples were obtained with aX´Pert PRO MPD Philips diffractometer (PANanalytical), equipped with a Ge (111) primary monochromator using CuKα1 (1.5406 Å) radiation. The X-ray tube was set at 45 kV and 40 mA and the measurements were carried out from 10° to 70° (2theta) for 12 minutes.

CO chemisorption analyses were performed under static volumetric conditions in a Micromeritics ASAP 2020 apparatus. Samples were reduced ex situ and transferred into an inert atmosphere. Prior to measurement samples were re-reduced in situ in $H_2$ at 300 °C and evacuated at 25 °C for 10 h. The chemisorption isotherm was obtained by measuring the amount of CO adsorbed between 10 and 600 mmHg at 35°C. After completing the initial analysis, the reversibly adsorbed gas was evacuated and the analysis repeated to determine only the chemisorbed amounts.

X-ray photoelectron spectra were collected using a Physical Electronics PHI 5700 spectrometer with non-monochromatic Al $K_\alpha$ radiation (300 W, 15 kV, and 1486.6 eV) with a multi-channel detector. Spectra of pelletized samples were recorded in the constant pass energy mode at 29.35 eV, using a 720 μm diameter analysis area. Charge referencing was measured against adventitious carbon (C 1*s* at 284.8 eV). A PHIACCESS ESCA-V6.0 F software package was used for acquisition and data analysis. A Shirley-type background was subtracted from the signals. Recorded spectra were always fitted using Gaussian-Lorentzian curves in order to determine the binding energy of the different element core levels more accurately. Reduced catalysts were stored in sealed vials with an inert solvent. The sample were prepared in a dry box under a $N_2$ flow and analyzed without previous treatment.

Temperature-programmed desorption (TPD) experiments were carried out to determine the acidity of the samples by using ammonia ($NH_3$-TPD) and the hydrogen activation capability was determined by using Hydrogen ($H_2$-TPD). For $NH_3$-TPD experiments, 80 mg of catalyst precur-

sor was reduced at atmospheric pressure using the same procedure described in the section 2.2. After flushing with helium and adsorption of ammonia at 100 °C, $NH_3$-TPD was performed using a helium flow and raising the temperature from 100 to 800 °C at a heating rate of 10 °C $min^{-1}$. Prior to raising the temperature, physisorbed ammonia was removed flushing with helium. For the $H_2$-TPD measurements 300 mg of catalyst precursor were reduced using the same procedure as described in section 2.2. The catalyst was cooled under flowing helium from the reduction temperature down to 100 °C and then exposed to $H_2$ gas with a flow of 60 mL $min^{-1}$ at 100 °C for 30 minutes, followed by flushing in argon for another 30 minutes in order to remove physisorbed hydrogen, and then heated in argon to 800 °C. The evolved gas was analyzed by online gas chromatography (Shimadzu GC-14A) equipped with a TCD.

Fourier transform infrared (FTIR) spectra of the samples after reduction and outgassing at 400°C as well as FTIR spectra of adsorbed CO were recorded with a Nicolet Nexus instrument, using a conventional cell connected to a gas-handling system. All spectra were obtained after subtraction of the spectrum corresponding to the degassed sample. Prior to adsorption, pressed disks of powder samples with a diameter of 1.5 cm of sample powders (ca.20 mg) were thermally treated within the cell at 400 ºC Under $H_2$ (67 kPa) for 1 h. CO adsorption (0.13 kPa) experiments were performed at -140 ºC and spectra were recorded in the range -140 to 10 ºC while degassing.

### *2.4. Catalytic Activity*

Dibenzofuran (DBF) was chosen as a model compound for the HDO reaction of bio-oil. Furan derivate compounds are common template molecules used to evaluate the catalyst performance in HDO reactions including dibenzofuran which is a very low reactive compound. The reactions were carried out in a high-pressure fixed-bed continuous-flow stainless steel catalytic reactor (9.1 mm in diameter and 230 mm in length). The concentration of the organic feed was in the range of 1-4 wt.% and decalin was used as solvent. The catalysts were reduced ex-situ and saved in a close vial containing cyclohexane to avoid oxidation. For the activity tests, an amount of 0.25 g of catalyst were used (particle size 0.85–1.00 mm) diluted with quartz sand to a total volume of 3 $cm^3$. Prior to the catalytic tests, the catalyst was left to dry overnight in a hydrogen flow of 100 mL $min^{-1}$ with a temperature ramp starting at 40 °C and finishing at 400°C with a heating rate of 3 °C $min^{-1}$. After drying and before catalytic testing, the catalysts were left in a nitrogen flow of 20 mL $min^{-1}$ at 40 °C to avoid oxidation. Catalytic activities were measured at 275 °C under a 0.1-3.0 MPa pressure, with a flow rate of $H_2$ of 100 mL $min^{-1}$ and with hourly space velocities (WHSV) in the range of 0.4 - 2.6 $h^{-1}$. The evolution of the reaction was monitored by collecting liquid samples every 60 minutes for 6 hours. A volume of 0.33 ml of product was col-

lected and diluted up to 1 ml volume with pure decalin and 20 µl of nonane were added as an internal standard. These samples were kept in sealed vials and subsequently analyzed by gas chromatography (Shimadzu GC-14B, equipped with a flame ionization detector and a capillary column, TBR-14, coupled to an automatic Shimadzu AOC-20i injector). In order to identify intermediates samples were also analyzed by CG-MS (MODEL) with a TBR-14 capillarity column.

The catalytic selectivity was calculated considering all the reaction products observed, biphenyl (BP), cyclohexylbenzene (CHB), tetrahydrodibenzofuran (THDBF), hexahydrodibenzofuran (HHDBF), 2-cyclohexylphenol (2-CHP), bicyclohexyl-2-en-3-ol (BCH-2-en-3-ol) and cyclopentylmethylcyclohexane (C-PE-ME-CH). Carbon balances are in the range of 1.00 +/- 0.05

The HDO conversion was calculated by the following equation;

$$HDO_{Conv.}(\%) = \frac{C_{DBF.Ini} - C_{DBF.Fin} - C_{Int}}{C_{DBF.Ini}} \times 100 \qquad (1)$$

where $C_{DBF.Ini}$ is the DBF concentration in the feed, $C_{DBF.Fin}$ is the DBF concentration in the HDO liquid product and $C_{IntHyd}$ is the concentration of O-containing intermediates (THDBF, HHDBF, 2-CHP, BCH-3-en-2-ol).

The turnover frequency was calculated using equation (2):

$$TOF = -\frac{F/W}{M} \times \ln(1 - X) \qquad (2)$$

where F is the molar rate of reactant (mol $min^{-1}$), W is the catalyst weight (g), X is the conversion and M is the mole of sites loaded (mol $g^{-1}$) calculated from CO-chemisorption. This formula was used because the conversions were close to 100% so were far from differential conditions, and an integral analysis was needed. This equation, in which -ln(1-X) substitutes for X assumes a pseudo first-order reaction which may be justified by the large excess of hydrogen.

In order to determine if internal diffusion is limiting the reaction the Weisz-Prater criterion can be used. It uses measured values of the rate of reaction to determine if the reaction suffers from problem of internal diffusion. Internal mass transfer effect can be neglected when the value of CWP is less than 1[16]. The detail of the calculations made is found as suplementary information (S1). All the values of $C_{WP}$ obtained under the experimental conditions studied were in the order of $10^{-2}$-$10^{-3}$. This indicates that internal mass transfer effects can be neglected at the conditions employed for this reactivity study.

## 3. Results and discussion

### *3.1. Catalytic study*

The HDO activity and selectivity of the reduced catalysts were investigated by using DBF as a model molecule present in bio-oil. Several experimental parameters were evaluated in order to better understand the reaction mechanism of the HDO reaction of DBF and to find the optimal experimental conditions to transform DBF into O-free products. Several types of products can be formed during HDO reaction, presented in Scheme 1, depending on the route followed. There is a hydrogenation pathway 1, in which oxygen removal is preceded by hydrogenation of benzene rings; a direct deoxygenation pathway 3, in which oxygen removal occurs by direct cleavage of bonds linking oxygen to aromatic carbons; and an intermediate pathway 2, in which oxygen removal is preceded by hydrogenation of one benzene ring only.

In the present work a further study to investigate the reaction mechanism of HDO of DBF on $Ni_2P$ and CoP catalysts is performed by changing several operational parameters; contact time, reaction pressure and $H_2$/DBF ratio feed.

#### 3.1.1 Contact time analysis

Contact-time experiments were carried out to improve the understanding of the reaction network and therefore the hydrogen gas volume flow and the feed (DBF in decalin) volume flow were adjusted. The hydrogen pressure, $H_2$/DBF molar ratio and the reaction temperature maintained constant. The catalytic results in terms of total conversion and HDO conversion are presented in Figure 1 in a contact time range of 1.8-12 s. It is observed that both total (dotted lines) and HDO conversion (solid lines) rise with increased contact time. Total conversion is always higher than HDO conversion, since the former only considers DBF transformation; instead, the later considers DBF transformation into O-free compounds. It is clearly seen that the longer the catalyst is in contact with the reactants the more of them can react and transform into oxygen free products. The $Ni_2P$ catalyst turns out to be more active than CoP, whereas only at low contact times CoP is slightly more active than $Ni_2P$. $Ni_2P$ catalyst presents the highest HDO conversion values at a contact time of 6 s, where the conversion values are reaching 98%. Instead, on CoP catalyst the highest value (80%) is attained at a contact time of 12 s. At low contact times the catalysts exhibit a low catalytic activity (less than 15% conversion). With regard of to the lower conversion value observed at very high contact time for $Ni_2P$ catalyst, in a recent work of A. Lino et al[19] about HDO of 2-MTHF on $Ni_2P$, these authors have observed a linear relationship in the plot of

conversion versus contact time. These author have pointed that in this situation each reactant molecule is reacting independently, meaning that each reactant molecule sees essentially a fresh surface. On $Ni_2P$, the linearity is maintained until a contact time of 6 s where the conversion is close to 100%. By increasing the contact time the conversion lowers perhaps to surface coverage with other organic species. If there were coverage, the rate of adsorption would be retarded by those species and therefore decreasing the conversion.

The reaction network is studied by observing the trends of product selectivity at different contact times. Figure 2 shows the product selectivity as a function of contact time for $Ni_2P$ catalyst and CoP catalyst, respectively. The products are classified into three groups; saturated oxygen-free cyclic compounds, unsaturated oxygen-containing cyclic compounds and furans.

At low contact times the intermediates tetrahydrodibenzofuran (THDBF) and hexahydrodibenzo-furan (HHDBF) are observed as products along with 2-cyclohexylphenol (2CHP) and bicyclo-hexyl-2-en-3-ol (BCH-2-en-3-ol). It should be noted that on $Ni_2P$, the selectivity to 2-CHP did not change obviously, and the selectivity to BCH-2-en-3-ol firstly increased and then decreased, indicating that BCH-2-en-3-ol is an intermediate for $Ni_2P$ catalyst. This is not the case for CoP one: as the contact time increased, the selectivities to 2-CHP and BCH-2-en-3-ol did not change monotonously.

By increasing the contact time the transformation of O-containing intermediates into O-free compounds occurs. Bicyclohexane (BCH) is the main O-free compound product formed in all reactions.

Based on the observation of formed intermediates and products and reviews of earlier studies [9,22], the reaction mechanism of HDO on CoP and $Ni_2P$ catalysts follows the hydrogenation pathway 1. In the first step one of the benzene rings in DBF is hydrogenated and the furan ring opens up:

DBF→THDBF→HHDBF→2-CHP

In the next step the second benzene ring is hydrogenated:

2-CHP→BCH-3-en-2-ol→BCHol

Then the oxygen removal takes place by dehydration and cycloalkane formation, which is the last step when both aromatic rings are completely saturated.

BCHol→BCH + C-PE-CH + C-PE-ME-CH

From these results it can be concluded that the catalysts have both metallic and acidic properties. They show good hydrogenation properties which can be explained by the high metallic disper-

sion and they also present acidic properties which shows in their hydroisomerization ability leading to C-PE-CH and C-PE-ME-CH. Moreover a contact time of 6 s seems to be adequate to assess the transformation of DBF into O-free products by following the route 1 presented in Scheme 1.

### 3.1.2 $H_2$ Pressure study

Another parameter evaluated was the reaction $H_2$ pressure, an important parameter in hydrogenation reactions. For this aim the reaction was carried out at three different $H_2$ pressures, 1, 15 and 30 bar, while the other parameters were kept constant; temperature 275 °C, $H_2$/DBF molar ratio 69 and the contact time 6 s. Figure 3 shows the total conversion and the HDO conversion as a function of the $H_2$ pressure. The plots of Figure 3 indicate that the activity is very low when the reaction is performed at atmospheric pressure (the conversion is below 5% with both catalysts). Nonetheless, $Ni_2P$ is more active than CoP at medium and high pressures. Moreover, both $Ni_2P$ and CoP are active at medium pressures with HDO degrees similar to those attained at 30 bar in the case of CoP. These results indicate that the reaction can be carried out at moderate pressures and that high pressures are not required to perform O-removal as in S- N- removal, where high pressures are always required. A higher $H_2$ pressure is beneficial also in hydrodeoxygenation as by increasing the pressure the thermodynamics would shift further towards complete conversion. However, too much $H_2$ interferes with the adsorption of reactants on the surface[19]. This could explain why the conversion is slightly higher at the 15 bar pressure compared to the 30 bar pressure for CoP catalyst. Wang et al[23] observed an improvement in DBF conversion via the hydrogenation pathway by increasing the pressure from 0.5 to 5.0 MPa on Pt/SBA-15 catalysts. In our case the excellent activity of metallic phosphides, even being highly active at medium pressures, should be highlighted in this type of reaction.

Considering the O-free product yield (Figure 4) at the different pressures, it is possible to observe that there is no major changes in product yield distribution by increasing the pressure from 15 to 30 bar in the case of the CoP sample, however, the $Ni_2P$ catalyst yielded greater amounts of BCH at high pressures. It is worth noting that the maximum yield of a certain intermediate was <4% in all experiments. At pressures of 15 and 30 bar the yield of the final product, BCH, is much higher for $Ni_2P$. These observations are consistent with the mechanism and the conclusion is that CoP catalyst is less active than $Ni_2P$.

### 3.1.3 $H_2$/DBF molar ratio study

With the aim to study how the reaction is influenced by different $H_2$/DBF molar ratios, the feed was prepared with three different compositions ($H_2$/DBF molar ratios of 34, 69 and 139). Figure 5 shows the total conversion and the HDO conversion as a function of $H_2$/DBF molar ratio.

The first thing observed is that the $Ni_2P$ catalyst is much more active than CoP, and also that the $Ni_2P$ sample is less affected by $H_2$/DBF molar ratios than the CoP catalyst. In fact, at low $H_2$/DBF molar ratios the activity of the $Ni_2P$ sample is close to that observed at high molar ratios. On the contrary the CoP sample shows a sharp increase in activity by increasing the $H_2$/DBF molar ratio. The highest conversion of all the experiments, when keeping the contact time at 6 s, is achieved at the highest $H_2$/DBF molar ratio for both catalysts.

The yields of the different reaction products for this set of experiments are depicted in Figure 6. It is observed that the $Ni_2P$ sample shows high yields to BCH (>80%) regardless the $H_2$/DBF molar ratio employed, which demonstrates its high efficiency to convert DBF into O-free compounds under poorer $H_2$ conditions. The CoP samples only attain high yields of BCH at high $H_2$/DBF molar ratios.

In fact, when the HDO conversion evolution with time on stream is observed (Figure 7), at low $H_2$/DBF molar ratio (Figure 7A), cobalt catalyst suffers from a fast deactivation after the first hour of reaction. Its initial HDO conversion is close to 80%, meanwhile after 6 h on stream the HDO conversion attained is down at 35%. However HDO conversion for the $Ni_2P$ sample under the same conditions slightly decreases and reaches the steady state after 6 hours with a conversion of 89%.Contrary and as expected, at $H_2$/DBF=139 (Figure 7.B) both catalysts are rather stable, which confirms previous statement; higher $H_2$ contents are required to improve the activity of CoP.

### 3.1.4. Intrinsic activity of the prepared sample-TOF number

In order to evaluate the intrinsic activity of $Ni_2P$ and CoP catalysts at the different conditions employed, TOF numbers were calculated according to Eq. 2 and is defined as the moles of reactant converted per mol of active sites per unit of time. This value gives information about the activity per active site. Table1 compiles the calculated TOF numbers for contact time, pressure effect and $H_2$/DBF effect experiments, respectively.

From this table, it is observed how the TOF number is higher for the $Ni_2P$ catalyst except at low contact time contact time. Moreover, the TOF number increases for the $Ni_2P$ catalyst when the contact time is increased up to 6 s, for longer contact times the TOF number decreases. However,

no great changes in TOF number are observed for the CoP sample, what could indicate that the activity per active site is hardly affected by changes in contact time; it only increases at the highest contact time studied. Contrary the $Ni_2P$ sample is much more sensitive to these changes with the TOF number increasing with about 400% from 1.8 to 6.0 s, in accordance to the sharp increase in the conversion. From $H_2$ pressure effect experiments it is observed that at low $H_2$ pressure, the activity per active site is very low for both samples. Nevertheless at 15 and 30 bar, the $Ni_2P$ sites are much more active than the CoP ones. Finally, $H_2$/DBF experiments also showed that the $Ni_2P$ sites had the highest activity, presenting much higher TOF values than the CoP samples. Wang et al.[23] tested Pt, Pd and Ru catalysts in HDO of DBF and the most active catalyst presented a TOF value, at 30% HDO conversion, lower than the TOF value presented by CoP catalysts at the same conversion value (15 bar), 0.42 $s^{-1}$ vs. 2.55 $s^{-1}$, respectively.

It should be highlighted that the TOF value reached under $H_2$-poor conditions (4 wt.%DBF) is the highest 23.7 $s^{-1}$ and much higher than those found in the literature for noble-metal based catalysts[22-24] .

### *3.2. Catalyst characterization*

The textural properties of the prepared catalysts are included in Table 2. As showed in this table, BET surface area of the $SiO_2$ support was 218 $m^2 g^{-1}$ and that of the fresh $Ni_2P$ and CoP catalysts in pellets form were 109 and 126 $m^2 g^{-1}$, respectively. The decrease in specific surface area indicates that pores are partly blocked due to the presence of phosphides particles on the support which partially impede the access of gas molecules[25, 26]. The textural properties of $Ni_2P$ and CoP prepared catalysts were similar.

The active phases formed after reduction were firstly evaluated from XRD experiments. $Ni_2P$ and CoP catalysts do not show any well-defined diffraction lines (diffractograms not shown here). This is due to the low metallic loading of the catalysts (5 wt.%) and because of the high dispersion of the active phase as observed in earlier studies[9] . The diffractogram of $Ni_2P$ shows some weak diffraction signals centred at 2θ (º) = 40.7, 44.6 and 55.0 and assigned to the $Ni_2P$ phase (PDF 01-089-4864). Meanwhile, CoP catalyst shows a very weak diffraction line located at 2θ (º) = 48.3 and assigned to the CoP phase (JCPDS No. 29-0497).

CO chemisorption capacity of the reduced catalysts provides with information about the number of surface metal atoms and gives an estimation of the number of active sites. Table 2 compiles the CO uptake at room temperature for cobalt phosphide and nickel phosphide catalysts. Both

samples chemisorb similar amounts of CO, i.e., the number of active sites is quite similar in both catalysts.

A more detailed information about the phases formed on the catalyst surface was obtained by XPS. The corresponding binding energies values are summarized in Table 3. Both, Ni 2*p* core level spectrum and Co 2*p* core level spectrum are decomposed into three contributions, i.e., three doublets containing the $2p_{3/2}$ and $2p_{1/2}$ components. The first contribution at lower binding energy is due to $Ni_2P$ (853.1 eV) and CoP phase (777.3 eV); the second contribution centered at 856.6 eV for $Ni_2P$ catalyst and at 780.7 eV for CoP samples is due to $Me^{2+}$ species; meanwhile, the third contribution observed is due to the shake-up satellite assigned in the literature to divalent species. The core level spectra of P 2*p* were also analyzed (See Fig S1, Supplementary Information) and decomposed. Both catalysts show two doublets (P $2p_{3/2}$-solid lines and P $2p_{1/2}$ dash lines) were observed indicating that, at least, two phosphorus species are present on the catalyst surface. The band close to 134.0 eV is due to phosphate species and the other band at 129.3 eV for $Ni_2P$ sample and at 129.0 eV for CoP one is due to the phosphide phase. No unreduced $HPO_3H^-$ species are observed, which could be a result of the high reduction temperature employed[31]. A much more detailed discussion of XPS spectra for these phases can be found in previous papers[27, 28].

Table 3 includes the percentage of phosphorous as $PO_4^{3-}$ and as phosphide ($Ni_2P$ or CoP). It is clearly seen the much greater amount of phosphate species on $Ni_2P$ rather than on CoP, indicating a surface enrichment of P in the former. In line with this, the corresponding surface atomic ratios indicate that the Ni/P molar atomic ratio is much lower than the expected values due to the formation of the $Ni_2P$ phase. On the contrary, for CoP sample, the Co/P ratio is higher than the expected stoichiometric value due to the presence of CoP which indicates that there is a greater concentration of metallic atoms on the surface.

These results are explained considering that the same amount of P-precursor has been added in both catalysts. Nonetheless $Ni_2P$ is a metallic rich phosphide and CoP is a stoichiometric phosphide, therefore more P is included into the CoP structure. Moreover the reduction temperature to form CoP is higher than that for $Ni_2P$, 700 ºC vs 620 ºC. Therefore it is expected thatat greater quantities of P are released during the reduction process of CoP. As a result, the remaining extra-P is expected to be higher in the $Ni_2P$ catalyst.

The acidic properties of the catalysts were measured by temperature-programmed desorption of ammonia ($NH_3$-TPD) between 100 and 800 ºC. Figure 8 shows the corresponding profiles while

Table 4 compiles the amount of $NH_3$ desorbed (μmol of $NH_3$ $g^{-1}$) for the reduced catalysts. By comparing both profiles and the data compiled in Table 3 one sees that the amount of $NH_3$ released is much higher on $Ni_2P$ than on CoP and $Ni_2P$ sample releases $NH_3$ molecules at temperatures lower than 400 ºC (weak acidity) while CoP sample releases $NH_3$ molecules at very high temperatures (550-700 ºC), indicating the presence of strong acid sites on this CoP sample. Previously the presence of both Lewis and Brönsted acid sites has been reported for the $Ni_2P$ catalyst[29]. Lewis acidity was ascribed to unreduced $Ni^{2+}$ and Brönsted acidity due to PO-H species. No much $Co^{2+}$ or $Ni^{2+}$ species are expected to be present here, due to both the high reduction temperature applied. Therefore, the acidity would be expected to come from PO-H groups. XPS data show that the $Ni_2P$ sample presents a surface enrichment of P species which could account for its higher acidity.

FT-IR spectra of the samples after reduction and outgassing at 400°C will also give information about the presence of surface hydroxyl groups. The corresponding spectra are represented in Figure 9. These clearly show a main band at 3742 $cm^{-1}$ due to stretching of isolated silanol species together with a weaker band centered at 3670 $cm^{-1}$ due to PO-H stretching modes, thus confirming that the acidity detected over these samples arises mainly from the Phosphorous-containing species. The frequency of this band is completely consistent with the frequency values reported for phosphoric acid supported on several oxides such as $Al_2O_3$, $SiO_2$, $ZrO_2$, forming hydrogenphosphate species[30, 31]. A shoulder at 3700 $cm^{-1}$ also seems to be present, which could be due to another kind of OH groups showing intermediate acidic properties, possibly some silanols affected by nearby phosphate species. Moreover, the intensity ratio $I_{3670}/I_{3742}$ for the two silanol and P-OH bands is higher in the $Ni_2P$ sample spectrum, as a further evidence that this catalyst shows an higher surface concentration of P-OH species, as it was previously suggested by XPS data, and also justifying the greater acidity presented by this catalyst. In line with this, IR analysis of adsorbed CO at liquid nitrogen temperature over $Ni_2P$ sample corroborates the presence of P-OH groups on this catalyst. The corresponding subtraction spectra are reported in Figure 10, in the CO stretching region the main bands of the spectrum are centered at 2187, 2158 and 2130 $cm^{-1}$, shoulder. The main band at 2158 $cm^{-1}$ is assigned to CO weakly interacting with surface OH groups[32] through H- bonds and this band is readily disappearing at decreasing CO coverage. Its assignation is also confirmed by the negative band appearing in the OH stretching region (inset) due to the consumption of isolated OH groups after interaction with CO. From these data it seems that silanols are involved first (highest frequency band), but also P-OH are interacting with CO which behaves as weak base (negative component at 2168 $cm^{-1}$). Decreasing

CO coverage leads to a partial restoring of silanols, but on the other hand the negative band due to P-OH group is still clearly detectable, thus the hydrogen bonding of CO with the surface hydroxy groups of hydrogenphosphate is significantly stronger than that with silanol, in agreement with P-OH higher acidic strength.

On the other hand the band detected at 2187 $cm^{-1}$ is due to carbonyls coordinated over Ni-ions, acting as Lewis acidic sites at the catalyst surface[29, 32]. Upon outgassing this band decreases in intensity and shifts towards higher frequencies, as expected. The weaker component at 2130 $cm^{-1}$ can be assigned to carbonyls coordinated over partially reduced Ni ions (possibly $Ni^{+}$), whereas only a very weak and broad absorption from 2050 to 2000 $cm^{-1}$ could be assigned to carbonyls coordinated over a very dispersed nickel metal phase[33]. The presence of some metallic nickel particles cannot be discarded, possibly arising from Ni ions strongly interacting with the support and not involved with P-species during reduction to form the phosphide phase.

As for the CoP sample, the strongest acidic sites detected by $NH_3$-TPD could be assigned to the Co ions unreduced still exposed at the catalyst surface. In order to ascertain this hypothesis we performed CO adsorption and indeed the IR spectrum recorded at room temperature, i.e. when the strong band due to H-bound CO is not detectable, shows a weak carbonyl band at 2200 $cm^{-1}$ which can be assigned to CO coordinated over Co ions (insert in Figure 10).

Finally, when testing a catalyst for hydrotreating reactions, it is important to consider its capability to activate hydrogen. To this end, $H_2$-TPD experiments on $Ni_2P$ and CoP reduced samples were performed and their corresponding profiles are shown in Figure 11. In general, the temperature at which H-species are released helps to understand the nature of these species. The $H_2$-desorption below 250 °C is ascribed to the adsorbed $H_2$ on metal Ni or Co sites, while the $H_2$ desorption between 250°C and 450°C is ascribed to the $H_2$ from the metal-support interface. Finally, desorption at higher temperatures is usually ascribed to $H_2$ spill over species. At first glance, when comparing the $H_2$-TPD profiles of the two different catalysts it is clear that the $Ni_2P$ catalyst desorbs greater amounts of hydrogen species, indicating a greater capacity to activate $H_2$ compared to CoP. Moreover, the $Ni_2P$ catalyst mainly desorbs hydrogen at low temperature, that is, coming from the metallic surface. Besides, greater amounts of H-spillover are also present on this catalyst. Literature data indicate that $H_2$-desorption at intermediate temperatures on $Ni_2P$ catalysts could be related to P-OH groups at the metal support interface[34] and catalysts with greater amount of P-OH groups desorbs a greater amount of $H_2$[35]. In fact, the $Ni_2P$ catalyst desorbs greater amounts of $H_2$ from both metal surface and metal-support interface, revealing the

greater capability of $Ni_2P$ to activate hydrogen and also the greater amount of P-OH present, contributing to $H_2$-desorption at intermediate temperatures.

### *3.3. Discussion*

Catalytic results have shown the greater activity of the $Ni_2P$ catalyst with regard to the CoP one. The most important results are that both catalysts show important conversion levels at medium pressure (15 bar) and that $Ni_2P$ catalyst is hardly affected by changes in the $H_2$/DBF ratio, meanwhile the CoP one requires greater amounts of hydrogen to be active.

The main cause for catalyst deactivation in HDO reactions is considered to be carbon deposition on the surface[20]. Brønsted acid sites are responsible for coke formation as they act as proton donors that form carbocations, therefore coking increases with increasing acidity of the catalyst. However the HDO reaction does require acidity and a balance should be obtained to have acid sites capable to activate oxygen containing molecules but whose strength will not be too strong to give rise to coke formation[36]. As stated before, the $Ni_2P$ sample, presents a higher amount of acid sites of weak nature, probably related to its higher amount of P-OH groups on the surface. The CoP sample presents an important concentration of very strong acid sites that could be responsible for coke formation[36], this could explain the low activity at low $H_2$/DBF molar ratio where the concentration of C-species is expected to be higher. By increasing the $H_2$ content in the feed, hydrogen acts as a cleaner hydrogenating C-species on the surface and the coke formation is minimized[37].

Another reason for catalyst deactivation is the formation of water during reaction. The water formed could interact with oxidized metal phosphide particles. It has been observed in a previous study[9] that $Ni_2P$ catalysts with an initial P/Ni atomic ratio of 2 or higher are more stable than those with the P/Ni atomic ratio of 1. The oxidation resistance of $Ni_2P$ phase under water molecules has been explained in the literature[38] by the dissociation of $H_2O$ on $Ni_2P$ surface (0 0 1) which generates O atoms that interact with both P and Ni atoms, but preferably with P. This leads to the formation of oxy-phosphide species with electron transfer from P to O. Hence P shows a ligand effect and the P species may inhibit the interaction of Ni with O, improving the oxidation resistance of $Ni_2P$. In a previous work, we observed this fact on $Ni_2P$ catalysts, that is, catalysts with greater P content were more resistant to deactivation due to $H_2O$ interacting presumably with P-species[9]. By looking at XPS and IR data, it is clearly seen how the $Ni_2P$ sample

has a higher P-concentration on the surface compared to CoP mainly in the form of P-OH. This could be another reason why $Ni_2P$ shows the highest activity of the two catalysts.

The better results obtained with $Ni_2P$ vs CoP is not only related to the higher intrinsic activity of $Ni_2P$ but also extra P-species that play an important role in these systems. Characterization results have evidenced the presence of much more P-on the surface of $Ni_2P$, mainly in the form of P-OH groups and as a consequence this catalyst possesses better acidity and $H_2$-desorption capacity, mainly at low temperature. P-species provide P-OH groups that can act as acid site and as a source of hydrogen species.

The role of P was also evaluated in CoP catalysts presenting different P/Co molar ratios and tested in the catalytic hydrodechlorination of chlorobenzene[37]. The most active catalysts were those containing P/Co>2 and showing better acidity values and greater amount of H-species from $H_2$-TPD measurements. In line with this, in a recent manuscript of Chen et al[39], it has been evaluated the promoting effect of water and oxygen pretreatment in the hydrodechlorination activity of $Ni_2P/SiO_2$. $H_2O$ or $O_2$ pretreatment increased the amount of P-OH groups on the surface and improved the catalytic response of these systems. So the activity of $Ni_2P$ was explained in terms of synergism between Ni atoms and P-OH groups.

## 4. Conclusions

The catalytic activity of Nickel and Cobalt phosphides on silica was tested in hydrodeoxygenation of DBF as a model oxygenate compound under different experimental conditions. The results obtained pointed out that the $Ni_2P$ catalyst is more active than the CoP one. Moreover it is less affected by hydrogen pressure changes and presenting very high conversion values even at low $H_2$/DBF molar ratios. Both catalysts perform the HDO reaction through the hydrogenation route: DBF→THDBF→HHDBF→2-CHP→BCH-3-en-2-ol→BCHol→BCH + C-PE-CH + C-PE-ME-CH. Characterization results have indicated that the better activity of the $Ni_2P$ phase is related to its greater intrinsic activity, and the greater presence of extra-P. Extra P-OH species can prevent metal phase oxidation; act as weak acid sites that can interact with O-species; but they can also act as H-donors to perform reaction, meanwhile spillover species could act as surface cleaners avoiding deactivation by coke formation.

The presented results seem to indicate that extra P-OH groups on $Ni_2P$ could be those governing the excellent results presented by the $Ni_2P$ phase. $Ni_2P$ sample should be considered a good candidate to be employed in hydrotreating units to perform HDO reactions.

## Acknowledgements

The National Spanish Project CTQ2012-37925-C03-03 of MINECO, FEDER funds and Junta de Andalucía project P12-RNM-1565 are acknowledged for financial support.

## References

1. J. S. M. Khanna, and D. Zilberman, *Handbook of Bioenergy Economics and Policy*, Springer, New York, NY, 2010.
2. A. Demirbas, *Prog. Energy Combust. Sci.*, 2007, **33**, 1-18.
3. Q. Bu, H. Lei, A. H. Zacher, L. Wang, S. Ren, J. Liang, Y. Wei, Y. Liu, J. Tang, Q. Zhang and R. Ruan, *Bioresour. Technol*, 2012, **124**, 470-477.
4. Q. Lu, W.-Z. Li and X.-F. Zhu, *Energy Convers. Manag*, 2009, **50**, 1376-1383.
5. T.-S. Kim, S. Oh, J.-Y. Kim, I.-G. Choi and J. W. Choi, *Energy* 2014, **68**, 437-443.
6. M. L. Honkela, T. R. Viljava, A. Gutierrez and A. O. I. Krause, *RSC Energy Environ. Ser.*, 2010, **2010**, 288–306.
7. M. Krár, S. Kovács, D. Kalló and J. Hancsók, *Bioresour. Technol.*, 2010, **101**.
8. S. Boullosa-Eiras, R. Lødeng, H. Bergem, M. Stöcker, L. Hannevold and E. A. Blekkan, *Catal. Today*, 2014, **223**, 44-53.
9. J. A. Cecilia, A. Infantes-Molina, E. Rodríguez-Castellón, A. Jiménez-López and S. T. Oyama, *Applied Catalysi B: Environmental*, 2013, **136-137**.
10. Y. Lee and S. Oyama, *J. Catal.*, 2006, **239**, 376-389.
11. P. Clark, *J. Catal.*, 2001, **200**, 140-147.
12. P. Clark, *J. Catal.*, 2002, **207**, 256–265.
13. X. Wang, *J. Catal.*, 2002, **208**, 321–331.
14. J. A. Cecilia, A. Infantes-Molina, E. Rodríguez-Castellón and A. Jiménez-López, *Journal of Catalysis*, 2009, **263**, 4-15.
15. J. A. Cecilia, A. Infantes-Molina, E. Rodríguez-Castellón and A. Jiménez-López, *Appl. Catal. B Environ.*, 2009, **92**, 100-113.
16. P. Bui, J. A. Cecilia, S. T. Oyama, A. Takagaki, A. Infantes-Molina, H. Y. Zhao, D. Li, E. Rodríguez-Castellón and A. Jiménez-López, *Journal of Catalysis* 2012, **294**, 184-198.
17. S. T. Oyama, T. Gott, H. Zhao and Y.-K. Lee, *Catalysis Today*, 2009, **143**, 94-107.
18. H. Y. Zhao, D. Li, P. Bui and S. T. Oyama, *Appl. Catal. A Gen.*, 2011, **391**, 305-310.
19. A. Iino, A. Cho, A. Takagaki, R. Kikuchi and S. T. Oyama, *J. Catal.*, 2014, **311**, 17-27.
20. P. M. Mortensen, J.-D. Grunwaldt, P. A. Jensen, K. G. Knudsen and A. D. Jensen, *Appl. Catal. A Gen.*, 2011, **407**, 1-19.
21. T. A. Le, H. V. Ly, J. Kim, S.-S. Kim, J. H. Choi, H.-C. Woo and M. R. Othman, *Chem. Eng. J.*, 2014, **250**, 157-163.
22. Y. Wang, Y. Fang, T. He, H. Hu and J. Wu, *Catal. Commun*, **12**, 1201–1205.
23. L. Wang, C. Li, S. Jin, W. Li and C. Liang, *Catal. Letters*, 2014, **144**, 809-816.
24. L. Wang, M. Zhang, M. Zhang, G. Sha and C. Liang, *Energy & Fuels*, 2013, **27**, 2209-2217.
25. S. Oyama, *J. Catal.*, 2002, **210**, 207-217.
26. T. Koranyi, Z. Vit, D. Poduval, R. Ryoo, H. Kim and E. Hensen, *J. Catal*, 2008, **253**, 119–131.
27. J. N. Kuhn, N. Lakshminarayanan and U. S. Ozkan, *J. Mol. Catal. A Chem*, 2008, **282**, 9–21.
28. D. Eliche-Quesada, J. Mérida-Robles, P. Maireles-Torres, E. Rodríguez-Castellón and A. Jiménez-López, *Langmuir*, 2003, **19**, 4985-4991.
29. J. A. Cecilia, A. Infantes-Molina, E. Rodrıíguez-Castellón and A. Jiménez-López, *Journal of Physical Chemistry C*, 2009, 17032-17044.
30. T. Armaroli, G. Busca, C. Carlini, M. Giuttari, A. M. R. Galletti and G. Sbrana, *J. Mol. Catal. A:Molecular* 2000, **151**, 233-243.
31. G. Busca, G. Ramis, V. Lorenzelli, P. F. Rossi, A. L. Ginestra and P. Patrono, *Langmuir*, 1989, **5**, 911–916.
32. G. Garbarino, V. Sanchez Escribano, E. Finocchio and G. Busca, *Applied Catalysis B: Environmental*, 2012, **113-114**, 281-289.
33. I. Rossetti, C. Biffi, C. L. Bianchi, V. Nichele, M. Signoretto, F. Menegazzo, E. Finocchio, G. Ramis and A. D. Michele, *Applied Catalysis B: Environmental*, 2012, **117–118**, 384-396.
34. F. Nozaki, T. Kitoh and T. Sodesawa, *Journal of Catalysis*, 1980, **62**, 286-293.

35. T. Guo, J. Chen and K. Li, *Chinese Journal of Catalysis*, 2012, **33**, 1080-1085.
36. S. Echeandia, B. Pawelec, V. L. Barrio, P. L. Arias, J. F. Cambra, C. V. Loricera and J. L. G. Fierro, *Fuel*, 2014, **117**, 1061–1073.
37. J. A. Cecilia, A. Infantes-Molina, E. Rodríguez-Castellón and A. Jiménez-López, *J. Hazard. Mater.*, 2013, **260**, 167-175.
38. P. Liu, J. A. Rodriguez, Y. Takahashi and K. Nakamura, *J. Catal.*, 2009, **262**, 294-303.
39. J. Chen, T. Guo, K. Li and L. Sun, *Catal. Sci. Technol.*, 2015.

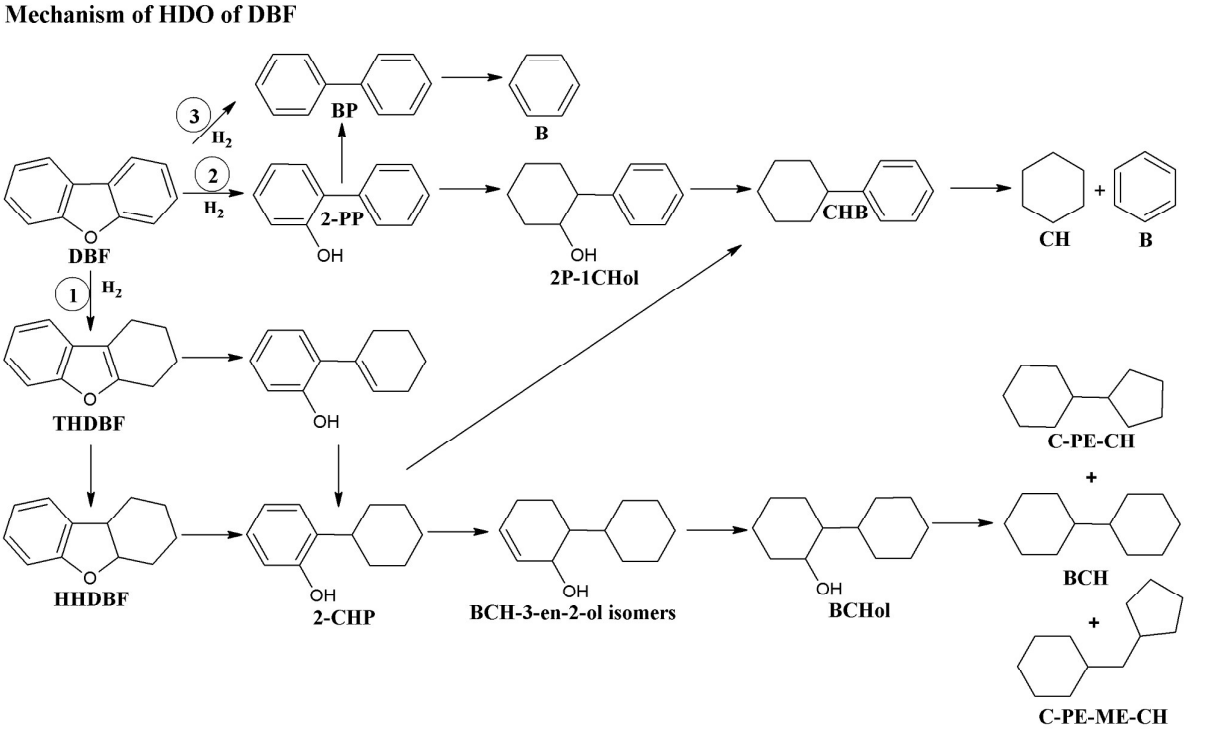


**DBF**: Dibenzofuran, **THDBF**: 2,3,4,9 Tetrahydrodibenzofuran, **HHDBF**: 2,3,4,4a,9,9a Hexahydrodibenzofuran, **2-CHP**: 2-cyclohexylphenol, **BCH-3-en-2-ol isomers**: 1-1'bi(cyclohexan)-3-en-2-ol, **BCHol**: By(cyclohexan)-2ol, **BCH**: Bicyclohexane, **C-PE-CH**: Cyclopentylcyclohexane, **C-PE-ME-CH**: (Cyclopentylmethyl)cyclohexane, **2-PP**: 2-phenylphenol, **2P-1CHol**: 2-Phenyl-1-cyclohexanol, **CHB**: Cyclohexylbenzene, **CH**: Cyclohexane, **B**: Benzene, **BP**: Biphenyl

Scheme 1. Mechanism of HDO of DBF

Table 1. TOF number for $Ni_2P/SiO_2$ and $CoP/SiO_2$ catalysts at T = 275 ºC, T.o.S.=6 h under different experimental conditions

| | $Ni_2P/SiO_2$ | $CoP/SiO_2$ |
|---|---|---|
| **Contact time (s)** | **TOF $x$ $10^2$ ($s^{-1}$) [a]** | |
| 1.8 | 1.69 | 3.33 |
| 2.4 | 2.67 | 2.27 |
| 3.6 | 6.68 | 1.40 |
| 6.0 | 8.42 | 2.18 |
| 12.0 | 4.30 | 3.15 |
| **$H_2$ Pressure (Bar)** | **TOF $x$ $10^2$ ($s^{-1}$)[b]** | |
| 1 | 0.33 | 0.14 |
| 15 | 7.95 | 2.55 |
| 30 | 8.42 | 2.18 |
| **$H_2$/DBF** | **TOF $x$ $10^2$ ($s^{-1}$)[c]** | |
| 34.3 | 23.7 | 3.01 |
| 69.2 | 8.42 | 2.18 |
| 139.0 | 6.09 | 2.93 |

[a] P= 30 Bar and $H_2$/DBF=69

[b] Contact time= 6 s and $H_2$/DBF=69

[c] P= 30 Bar and Contact time= 6 s

Table 2. Textural Properties[b] and CO Chemisorption[c] properties of the prepared samples

| | $S_{BET}$[b] ($m^2\ g^{-1}$) | $V_p$[b] ($cm^3\ g^{-1}$) | CO Chemisorption[c] ($\mu mol\ g^{-1}$) |
|---|---|---|---|
| Support $SiO_2$ | 218 | 0.52 | |
| $Ni_2P$ Pellets | 109 | 0.57 | 32.9 |
| CoP Pellets | 126 | 0.67 | 36.7 |

Table 3. Binding energy (eV) of core electrons and surface atomic ratios of fresh CoP and $Ni_2P$ catalysts

| Sample | Binding energy (eV) | | | | Atomic ratio | |
|---|---|---|---|---|---|---|
| | Ni $2p_{3/2}$/Co $2p_{3/2}$ | | P $2p_{3/2}$ | | Me/P | Me/Si |
| CoP | $Co^{2+}$ | CoP | $PO_4^{3-}$ | CoP | 1.65 | 0.04 |
| | 780.7 | 777.3 | 134.1 (48.6)* | 129.0 (51.4)* | | |
| $Ni_2P$ | $Ni^{2+}$ | $Ni_2P$ | $PO_4^{3-}$ | $Ni_2P$ | 0.41 | 0.01 |
| | 856.6 | 853.1 | 134.4 (25.5)* | 129.3 (74.5)* | | |

*In parenthesis the percentage of each specie

Table 4. Quantity of $NH_3$ released (μmol $g^{-1}$) from $NH_3$-TPD experiments

| Catalyst | μmol $NH_3$ $g^{-1}$ | | | | | |
|---|---|---|---|---|---|---|
| | Temperature (ºC) | | | | | |
| | Total | 100-200 | 200-300 | 300-400 | 400-500 | 500-800 |
| $Ni_2P$ | 481 | 155 | 202 | 98 | 20 | 6 |
| CoP | 211 | 57 | 71 | 35 | 8 | 41 |

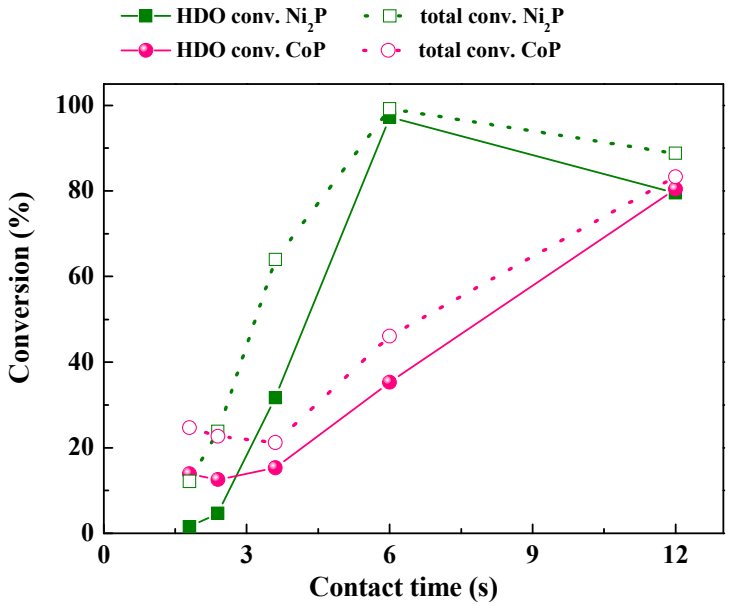


Figure 1. Total conversion and HDO conversion of DBF on $Ni_2P/SiO_2$ and $CoP/SiO_2$ as a function of contact time. Experimental conditions: T = 275 ºC; P = 30 Bar; $H_2$/DBF ratio 69; T.o.S= 6 h

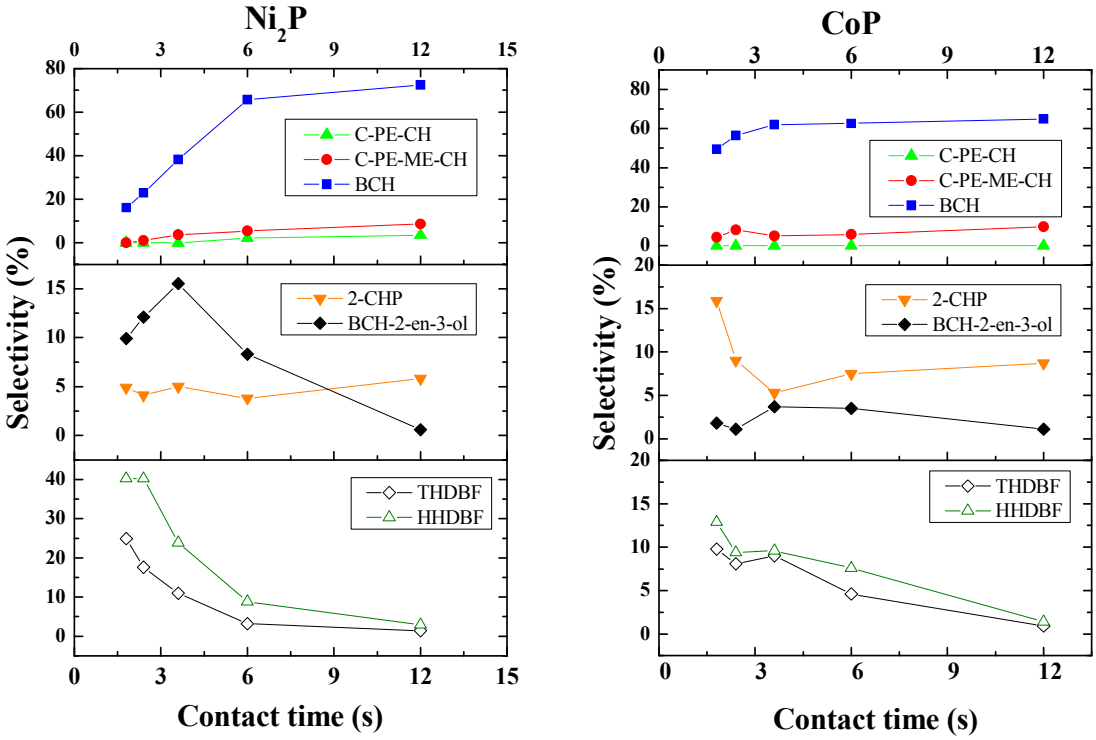


Figure 2. Product selectivity on $Ni_2P/SiO_2$ and $CoP/SiO_2$ as a function of contact time. Experimental conditions: T = 275 ºC; P = 30 Bar; $H_2$/DBF molar ratio 69; T.o.S= 6 h

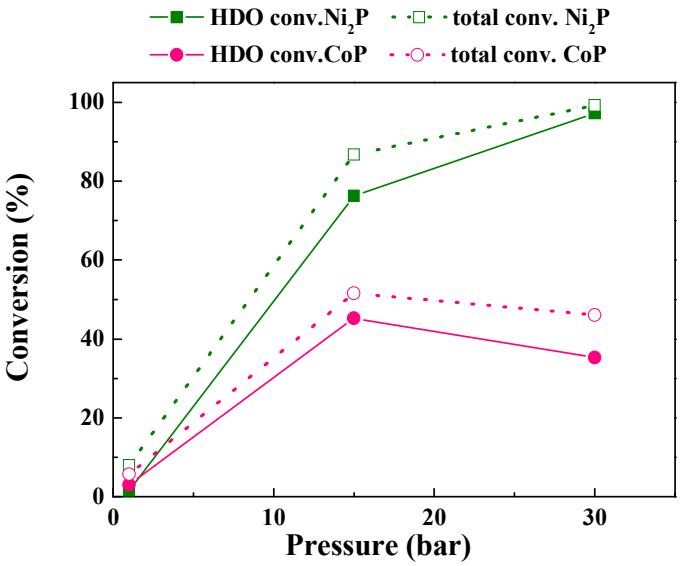


Figure 3. Total conversion and HDO conversion as a function of reaction pressure for $Ni_2P/SiO_2$ and $CoP/SiO_2$ catalyst. Experimental conditions: T = 275 ºC; contact time 6 s; $H_2$/DBF molar ratio 69; T.o.S= 6 h

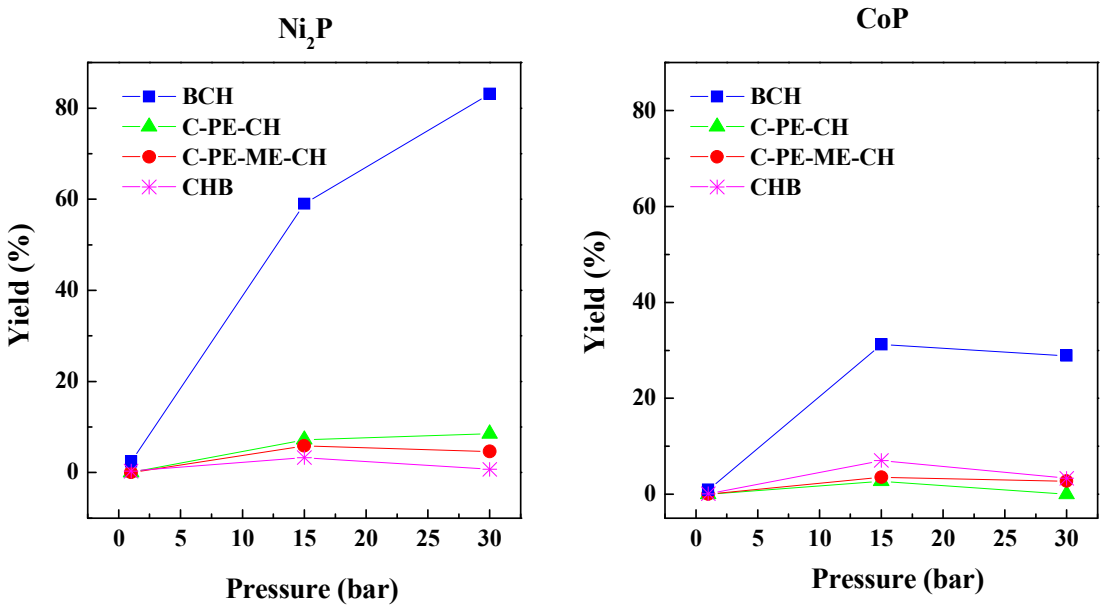


Figure 4. Yield distribution of the products as a function of $H_2$ pressure for $Ni_2P/SiO_2$ and $CoP/SiO_2$ catalyst. Experimental conditions: T = 275 ºC; contact time 6 s; $H_2$/DBF molar ratio 69; T.o.S= 6 h

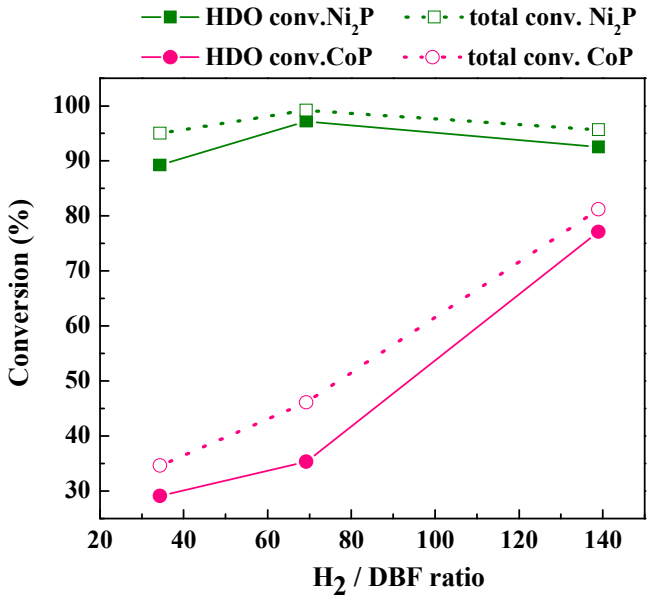


Figure 5. Total conversion and HDO conversion as a function of $H_2$/DBF molar ratio for $Ni_2P/SiO_2$ and $CoP/SiO_2$ catalysts. Experimental conditions: T = 275 ºC; P = 30 bar; contact time 6 s; T.o.S.= 6 h

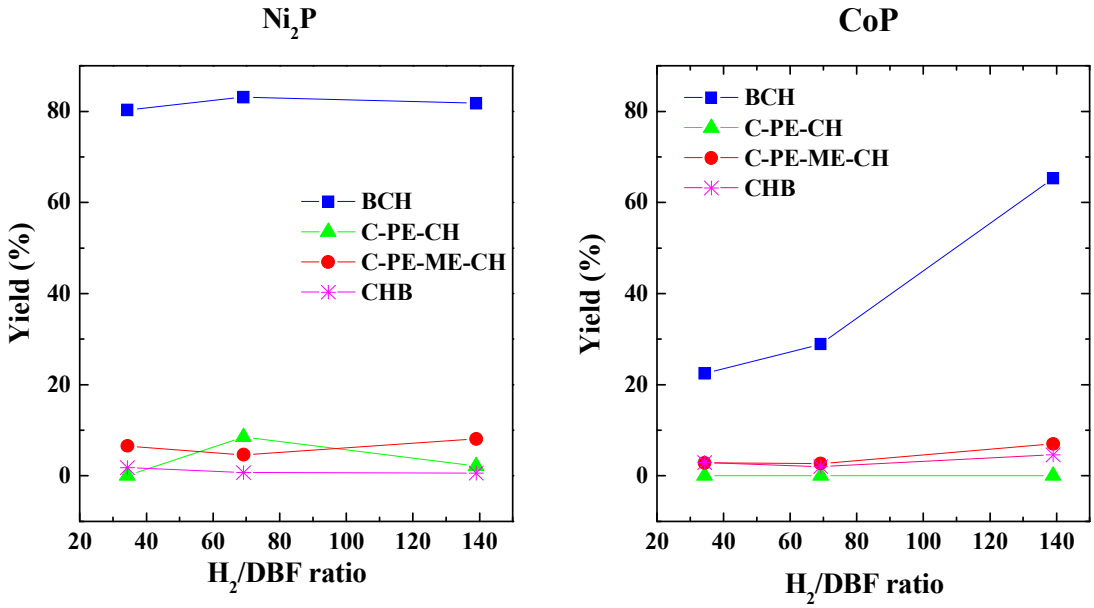


Figure 6. Yield distribution of the products as a function of $H_2$/DBF molar ratio for $Ni_2P/SiO_2$ and $CoP/SiO_2$ catalysts. Experimental conditions: T = 275 ºC; P = 30 Bar; contact time 6 s; T.o.S.=6 h

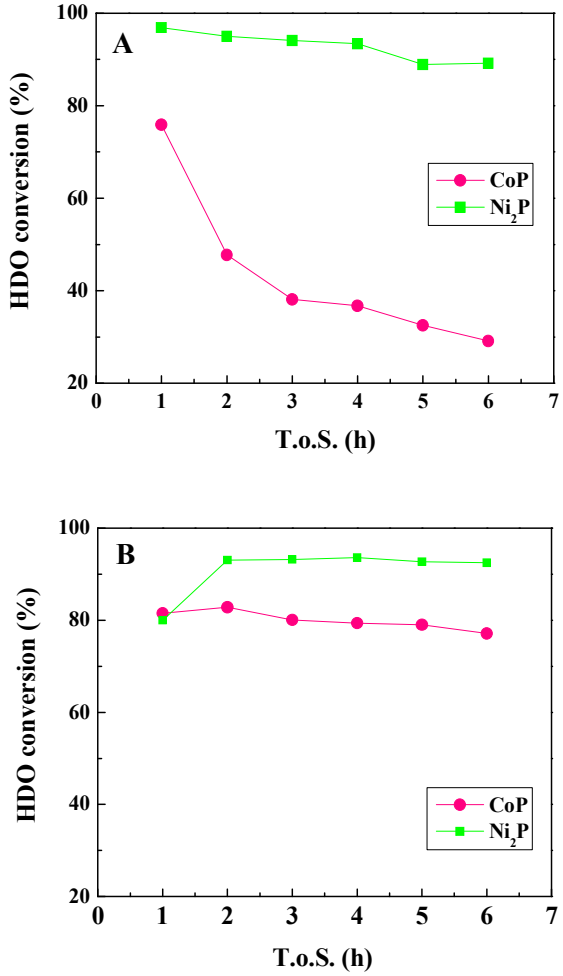


Figure 7. Evolution of conversion as a function of time on stream for $Ni_2P/SiO_2$ and $CoP/SiO_2$ catalysts tested at two different $H_2$/DBF molar ratios, A) 34 and B) 139. Experimental conditions: T = 275 ºC; P = 30 bar; contact time 6 s; T.o.S. = 6 h

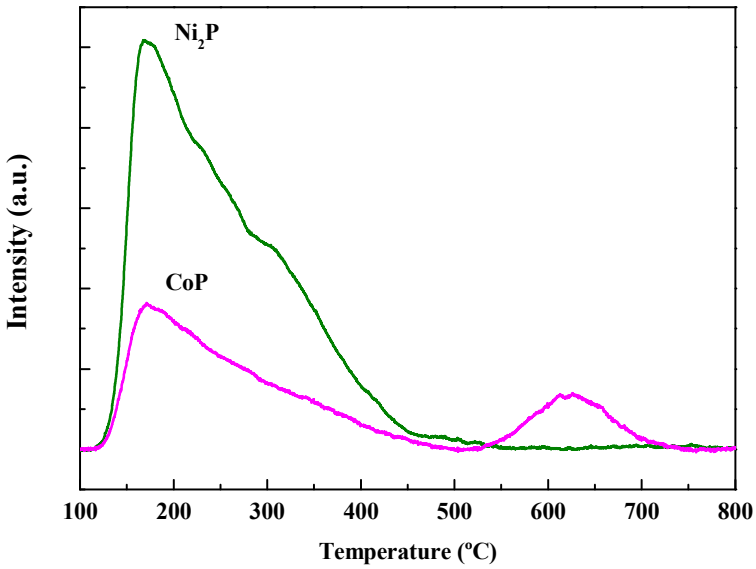


Figure 8. $NH_3$-TPD profiles of CoP and $Ni_2P$ catalysts

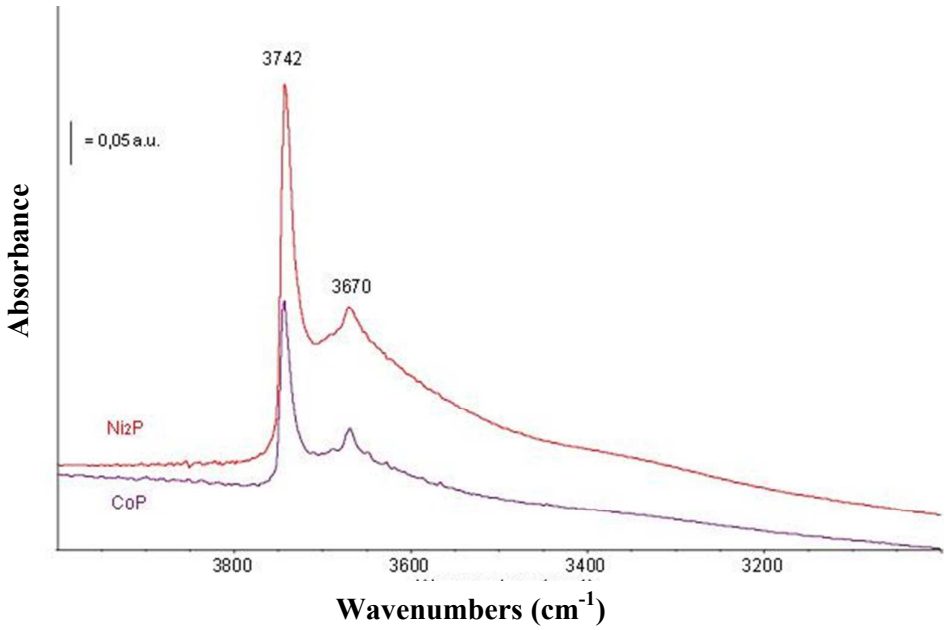


Figure 9. FT IR spectra of $Ni_2P$ and CoP samples after activation at 450°C. OH stretching region

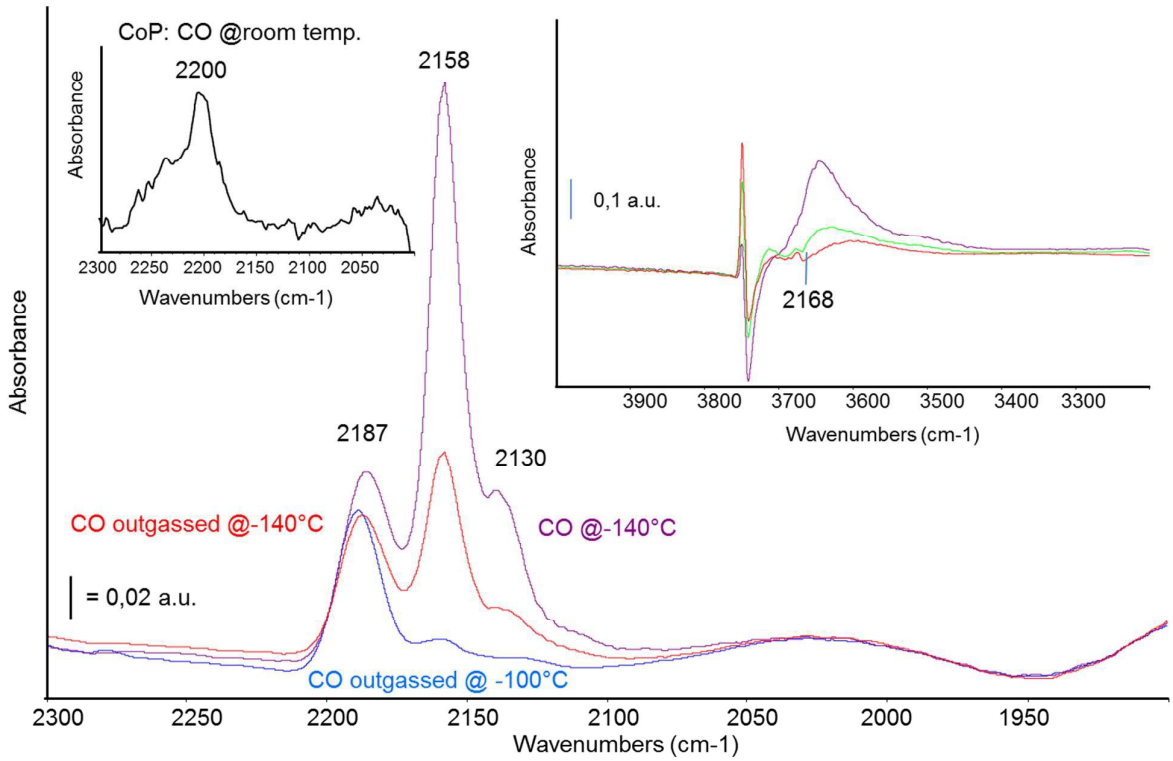


Figure 10. FT IR subtraction spectra of surface species arising from CO adsorption and outgassing at liquid nitrogen temperature on $Ni_2P$ catalyst and CO adsorption on CoP at room temperature. The activated surface has been subtracted. Inset: OH stretching region

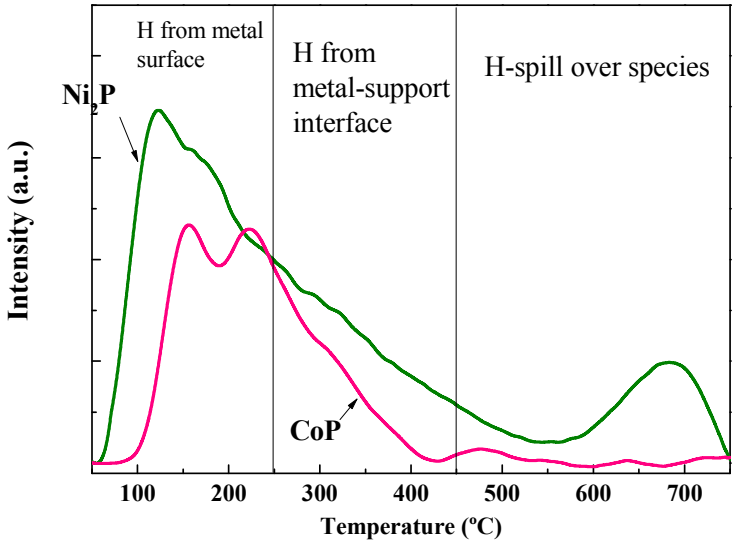


Figure 11. $H_2$-TPD profiles of CoP and $Ni_2P$ catalysts